ACADEMIC PRESS

Available online at www.sciencedirect.com

SCIENCE DIRECT®

Journal of Solid State Chemistry 171 (2003) 396–400

JOURNAL OF SOLID STATE CHEMISTRY

http://elsevier.com/locate/jssc

Luminescence and energy transfer of organically modified silica xerogels (OMSX) doped and undoped with Eu^{3+} and Tb^{3+}

Yinhua Han and Jun Lin*

Key Laboratory of Rare Earth Chemistry and Physics, Changchun Institute of Applied Chemistry, Chinese Academy of Sciences, 159 Renmin Street, Changchun 130022, People's Republic of China

Received 8 April 2002; received in revised form 15 July 2002; accepted 27 July 2002

Abstract

Organically modified silica xerogels (OMSX) and Eu^{3+} (Tb^{3+})-doped OMSX were prepared by the reaction of (3-aminopropyl) triethoxysilane (APS) with 3-isocyanatepropyltriethoxysilane (ICPTES) followed by the subsequent hydrolysis and condensation in the presence of Eu^{3+} (Tb^{3+}) via sol–gel method, which were characterized by FT-IR, XRD, fluorescence excitation and emission spectra. The as-formed OMSX shows a strong blue emission with the maximum excitation and emission wavelength at 351 and 420 nm, respectively. Due to the spectral overlap between the emission band of OMSX and $f-f$ absorption lines of Eu^{3+} and Tb^{3+} in the UV-blue region, an energy transfer was observed from OMSX host to Eu^{3+} and Tb^{3+} in OMSX/Eu^{3+} and OMSX/Tb^{3+}, respectively. Excitation at 350–360 nm resulted in a very weak emission around 420 nm from OMSX host and strong emission of Eu^{3+} and Tb^{3+} in OMSX/Eu^{3+} and OMSX/Tb^{3+}, respectively. The emission spectra of Eu^{3+} and Tb^{3+} consist of $^5D_0-^7F_J$ ($J = 0, 1, 2, 3, 4$) and $^5D_4-^7F_J$ ($J = 6, 5, 4, 3$), respectively. Furthermore, the predicted structure of OMSX/Eu^{3+} and OMSX/Tb^{3+} is presented.

Keywords: Luminescence; Energy transfer; Europium; Terbium; Silica xerogel

1. Introduction

Sol–gel derived silica gel (aerosol or xerogel) is of great importance based on its wide applications in optics, catalysts, sensors and solar energy collectors [1–4]. Organic dyes [5] and rare-earth ions [6–8] have been incorporated into the microporous silica gel, which is generally considered to possess an optically inert framework. However, the sol–gel derived silica gel is not optically inert, but optically active, i.e., it shows luminescence under UV excitation [9,10]. Of particular interest and importance is that, a new class of stable and efficient white photoluminescent silicate materials has been obtained from an alkoxysilane and a carboxylic acid through sol–gel route [11,12]. Other workers have reported that the sol–gel derived undoped urea contains cross-linked organic-inorganic xerogels which display strong blue-light emission [13].

In this paper we describe the luminescence and energy transfer properties of an organically modified silica xerogel doped and undoped with the rare-earth ions Eu^{3+} and Tb^{3+}. The organically modified silica xerogels were prepared by the reaction of two kinds of silane coupling agents, (3-aminopropyl) triethoxysilane (APS) with 3-isocyanatepropyltriethoxysilane (ICPTES), which shows a strong blue emission. It is of great interest to note that an energy transfer occurs from the silica xerogel host to the doped Eu^{3+} and Tb^{3+}.

2. Experimental

The undoped organically modified silica xerogels were prepared by the reaction of two silane coupling agents. Typically, 0.65 mL (3-aminopropyl) triethoxysilane (APS, C.P., produced by Gaizhou Chemical Plant, Liaoning) was dissolved in 3 mL ethanol with stirring. Then 0.65 mL 3-isocyanatepropyltriethoxysilane (ICPTES, Aldrich) was added to this solution in a fume cupboard. The flask was sealed and the solution

---

*Corresponding author. Fax: +86-431-5698041.
E-mail address: jlin@ns.ciac.jl.cn (J. Lin).

doi:10.1016/S0022-4596(02)00220-7

was stirred overnight in the presence of 0.5 mL H_2O, resulting in the formation of solid silica xerogel. The xerogel was dried at 120°C for 2 days.

The Eu^{3+}/Tb^{3+}-doped silica xerogels were prepared by dissolving Eu_2O_3/Tb_4O_7 with HNO_3, into which a small amount of ethanol was added. The concentration of Eu^{3+} and Tb^{3+} is 10 mol% of the OMSX in the host. The pH value of the solution was adjusted to 6–7. Then the mixed solution of APS and ICPTES was added to the above solution under stirring. The resulting sol was poured into a plastic bottle until solidification occurred to form transparent xerogels. The reaction processes and the predicted structures for the products are schematically shown in Fig. 1.

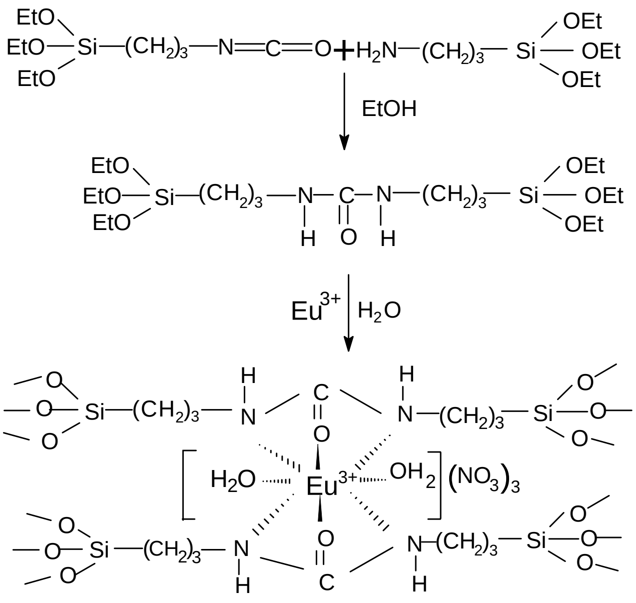

Fig. 1. The reaction process of ICPTES with APS and the predicted structure for OMSX/Eu^{3+}.

Photoluminescence excitation and emission spectra were measured on an SPEX-Florolog-2T2 spectrofluorometer equipped with a 450 W xenon lamp as the excitation source. FT-IR spectra were measured with FTS 135 (USA, BIO-RAD Company) infrared spectrophotometer over the range 4000–400 cm^{-1}. X-ray powder diffraction (XRD) measurements were performed on a Rigaku D/max-IIB X-ray diffractometer with Cu$K\alpha$ ($\lambda = 0.15405$ nm) radiation (40 kV, 20 mA). All measurements were performed at room temperature.

3. Results and discussion

Fig. 2 shows the FT-IR spectra of the starting materials ICPTES (a), APS (b) and their reaction produced OMSX (c). For ICPTES, the FT-IR spectrum contains the absorption peaks located at 2978, 2883 cm^{-1} (asymmetric $–CH_2$ stretching and symmetric $–CH_2$ stretching), 2270, 1720 cm^{-1} (asymmetric $–N=C=O$ stretching and symmetric $–N=C=O$ stretching), 1386 cm^{-1} ($–CH_2$ bending), 1195 cm^{-1} (Si–CH_2 stretching), 1081, 950 cm^{-1} (asymmetric Si–OEt stretching), 780 cm^{-1} (symmetric Si–OEt stretching) and 450 cm^{-1} (bending of Si–OEt). The FT-IR spectrum of APS is similar to that of ICPTES, except that the absorption of $–NH_2$ group at 1577 cm^{-1} replaces the absorption of $–N=C=O$ group at 2270, 1720 cm^{-1}. For the OMSX, the FT-IR spectrum is also similar to the starting materials ICPTES and APS to some extent, but the absorption of $–N=C=O$ group disappears completely and a new peak at 1642 cm^{-1} due to amide –

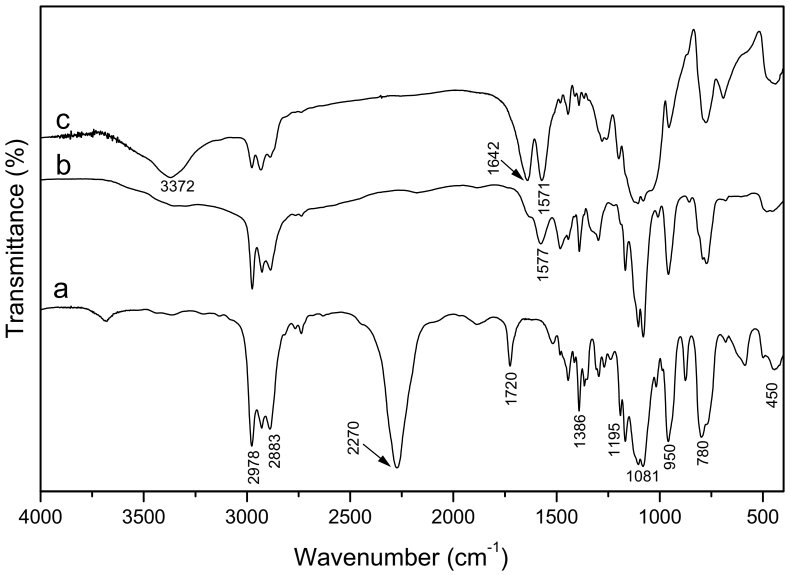

Fig. 2. FT-IR spectra of ICPTES (a), APS (b) and the OMSX (c).

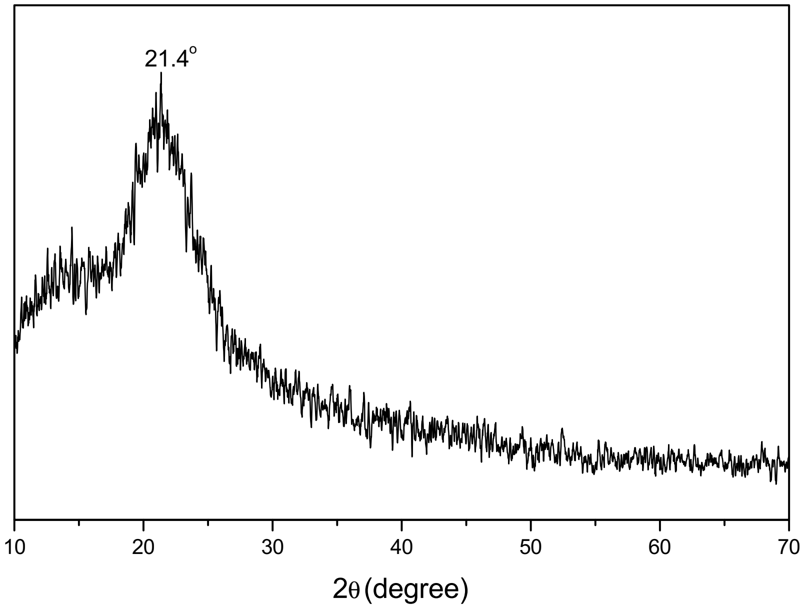

Fig. 3. X-ray powder diffraction pattern for OMSX.

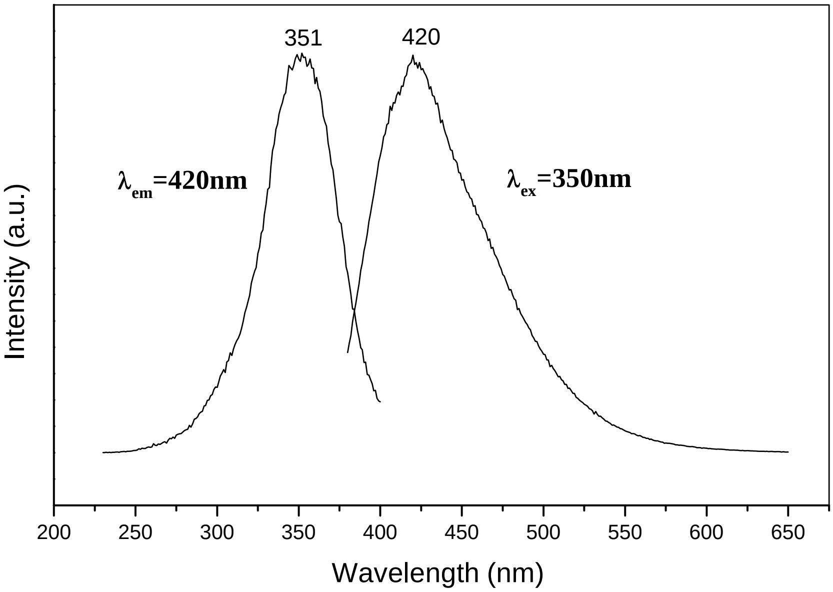

Fig. 4. Excitation (left) and emission (right) spectra of OMSX.

CONH group presents. The broad band at 3372 cm^{-1} is due to –NH vibration in the –CONH group. This results from the reaction of –NH_2 group in APS with –N=C=O group in ICPTES, as shown in Fig. 1. The XRD pattern of the as-formed OMSX only shows a broad band at $2\theta = 21.4°$, which is characteristic for amorphous silica, as shown in Fig. 3.

The as-formed OMSX shows a strong blue emission under ultraviolet (360 nm) excitation, which can be seen clearly with eyes. Fig. 4 presents the excitation and emission spectra of OMSX. The excitation spectrum consists of a broad band ranging from 250 to 500 nm with a maximum at 351 nm, and the corresponding emission spectrum contains an asymmetric broad band ranging from 350 to 550 nm with a maximum at 420 nm. The Stokes shift amounts to 4700 cm^{-1}. It is well-known that the Stokes shift, defined as the energetic difference between the maximum of the excitation spectrum and related maximum of the emission spectrum, is strongly connected with the electron-phonon coupling [13]. The Stokes shift for the luminescence of the OMSX is small (4700 cm^{-1}) and there is a strong overlap between the excitation and emission spectra. This suggests that there is a strong self-absorption for the luminescence of

OMSX, i.e., energy transfer takes place from one emission center to another.

The origin of the luminescence in sol–gel derived silica gels has not been well understood yet. Three possible mechanisms, i.e., defect mechanism [14], charge transfer mechanism [9] and carbon impurity mechanism [11,12], have been proposed to explain the luminescent phenomena in the sol–gel derived silica gels. It is believed that the carbon impurity mechanism dominates the blue emission in OMSX [11,12], i.e., the emission is considered to be from the introduction of carbon impurities in the –O–Si–O– network by forming –O–C–O– or –Si–C-bonds.

Fig. 5 shows the excitation and emission spectra of OMSX/Eu^{3+} (a) and OMSX/Tb^{3+} (b). In Fig. 5(a), monitored with the red emission of Eu^{3+} $^5D_0-^7F_2$ transition at 617 nm, the excitation spectrum consists of the f-f transition lines of Eu^{3+} at 319, 361, 381, 394, 416, 465 nm, which seem to be superimposed on a broad band from 300 to 450 nm. This broad band is due to the excitation of the OMSX host, as shown in Fig. 4. The same situation holds for the excitation spectrum of

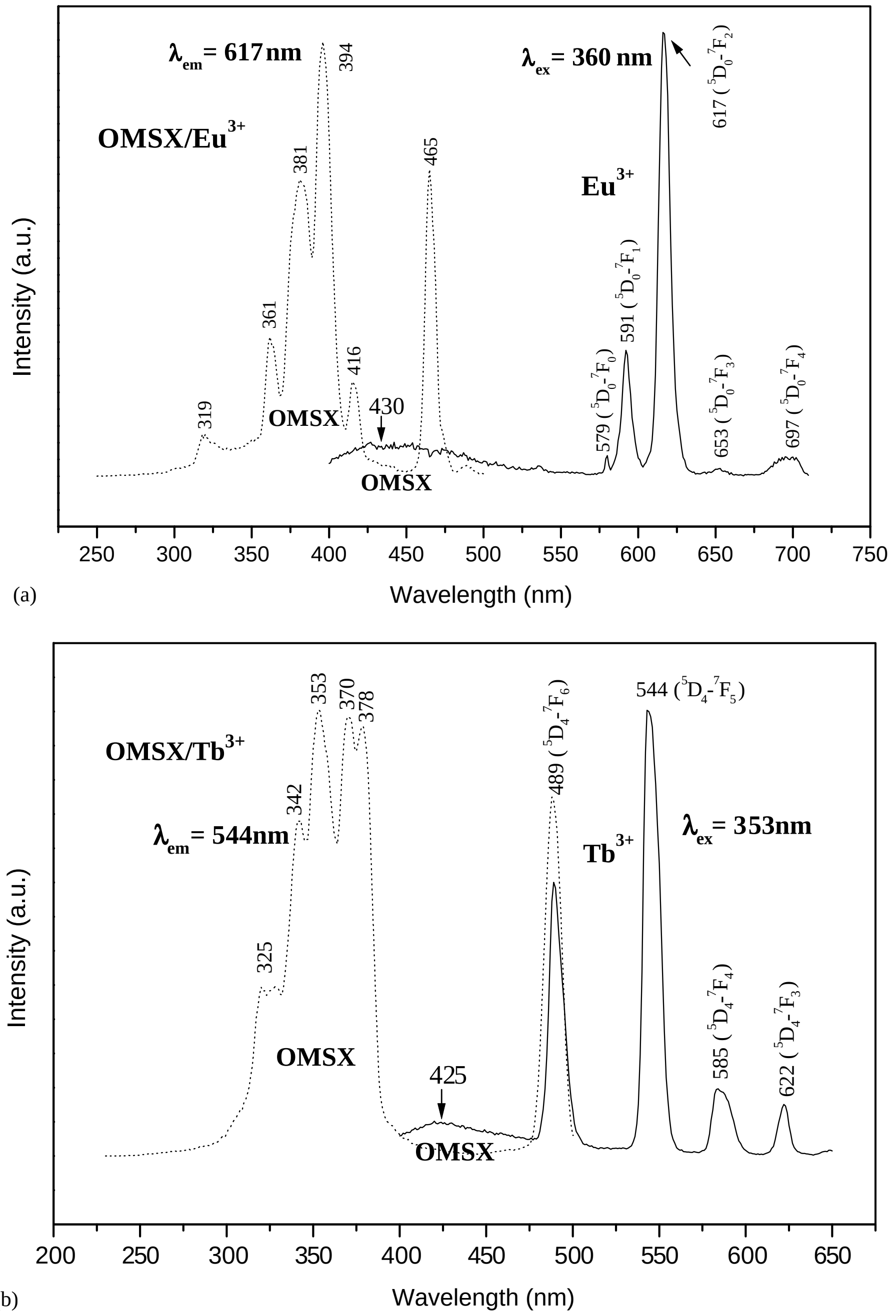

Fig. 5. Excitation (dot line) and emission (solid line) spectra for OMSX/Eu^{3+} (a) and OMSX/Tb^{3+} (b).

OMSX/Tb^{3+} (Fig. 5b left, dot line). In this case the monitored emission light is Tb^{3+} $^5D_4-^7F_5$ at 544 nm, and the excitation band of OMSX host is more obvious. The presence of the strong excitation band of OMSX in the excitation spectra of Eu^{3+} and Tb^{3+} indicates that an energy transfer occurs probably from the OMSX host to Eu^{3+} and Tb^{3+} in OMSX/Eu^{3+} and OMSX/Tb^{3+}, respectively. Excitation at 350–360 nm yields very weak band emission of OMSX host from 400 to 500 nm and strong line emission of Eu^{3+} $^5D_0-^7F_J$ ($J=0, 1, 2, 3, 4$) in OMSX/Eu^{3+} and Tb^{3+} $^5D_4-^7F_J$ ($J = 6, 5, 4, 3$) in OMSX/Tb^{3+}, respectively. Because there exist some $f-f$ transition excitation lines for Eu^{3+} and Tb^{3+} in the range of 350–360 nm, both the energy transfer from OMSX host and their self-excitation have contributions to the strong emission of Eu^{3+} and Tb^{3+}, and it is difficult to calculate the energy transfer efficiency in OMSX/Eu^{3+} and OMSX/Tb^{3+} systems. The strongest emission lines of Eu^{3+} and Tb^{3+} are located at 617 nm (red, $^5D_0-^7F_2$) and 544 nm (green, $^5D_4-^7F_5$), respectively. Luminescence from higher excited states such as $^5D_1$ of Eu^{3+} and $^5D_3$ of Tb^{3+} is not observed, indicating a very efficient non-radiative relaxation from $^5D_1$ to $^5D_0$ for Eu^{3+} and $^5D_3$ to $^5D_4$ for Tb^{3+} due to the high vibration energy (3372 cm^{-1} of –NH, 1090 cm^{-1} of Si–O–si, as shown in Fig. 2c) in the OMSX host. The cross relaxation between $^5D_3-^5D_4$ and $^7F_0-^7F_6$ of two Tb^{3+} ions also plays an important role in quenching the emission from $^5D_3$ [15]. The presence of Eu^{3+} $^5D_0-^7F_0$ transition, and the dominated hypersensitive $^5D_0-^7F_2$ transition, indicates a low symmetry local environment for Eu^{3+}(and Tb^{3+}) in the OMSX host [16].

The energy transfer from OMSX to Eu^{3+} and Tb^{3+} can be explained by the spectral overlap. The emission spectrum of OMSX is a broad band ranging from 350 to 550 nm, which overlaps with most of the excitation lines of eu^{3+} and Tb^{3+}, such as 361, 381, 394, 416, 465 nm for Eu^{3+} and 342, 353, 370, 378 and 490 nm for Tb^{3+}. As a result, the emission energy of OMSX can be absorbed by the Eu^{3+} and Tb^{3+} via their $f-f$ excitation transitions and energy transfer from OMSX to Eu^{3+} and Tb^{3+} takes place. Because the emission of OMSX, Tb^{3+} and Eu^{3+} is in the blue, green and red region respectively, it is possible to obtain a white light by suitably doping both Eu^{3+} and Tb^{3+} in OMSX host. This study is under way and will be reported later.

4. Conclusions

An organically modified silica xerogel (OMSX), derived from the interaction of two silane coupling agents APS and ICPTES by sol–gel process, shows a strong blue emission from 350 to 550 nm with a maximum at 420 nm under longer ultraviolet excitation. Eu^{3+} and Tb^{3+}-doped OMSX shows the characteristic strong red emission of Eu^{3+} (617 nm, $^5D_0-^7F_2$) and green emission of Tb^{3+} (544 nm, $^5D_4-^7F_5$) respectively, and there exists a possible energy transfer from the OMSX host to Eu^{3+} and Tb^{3+}.

Acknowledgments

This project is financially supported by the foundation of “Bairen Jihua”of Chinese Academy of Sciences, the Outstanding Youth Fund of Jilin Province (20010103), the National Natural Science Foundation of China (20271048, 50225205) and Personnel and Educational Ministry of China.

References

[1] K.I. Jensen, J. Non-Cryst. Solids 145 (1992) 237.
[2] S. Otto, R. Wolfbeis, I. Reisfeld, Oehme, Struct. Bonding 85 (1996) 51.
[3] C. Houng-Van, B. Pommier, R. Harivololona, P. Pichat, J. Non-Cryst. Solids 145 (1992) 250.
[4] L.L. Hench, J.L. Nogues, in: L.C. Klein, (Ed.), Sol–Gel Optics Processing and Application, Kluwer, Dordrecht, 1994, p. 59.
[5] R. Reisfeld, C.K. Jorgensen, Struct. Bonding 77 (1992) 207.
[6] M.A. Zaitoun, T. Kim, C.T. Lin, J. Phys. Chem. B 102 (1998) 1122.
[7] L.D. Carlos, R.A. Sa Ferreira, Phys. Rev. B 14 (1999) 10042.
[8] E. Coroncillo, B. Viana, P. Escribano, C. Sanchez, J. Mater. Chem. 8 (1998) 507.
[9] J. Garcia M., M.A. Mondragon, C. Tellez, S.A. Campero, V.M. Castano, Mater. Chem. Phys. 41 (1995) 15.
[10] M.R. Ayers, A.J. Hunt, J. Non-Cryst. Solids 217 (1997) 229.
[11] W.H. Green, Khoa P. Le, J. Grey, Tiffany T. Au, M.J. Sailor, Science 276 (1997) 1826.
[12] V. Bekiari, P. Lianos, Langmuir 14 (1998) 3459.
[13] R.A. Sa Ferreira, L.D. Carlos, V. de Zea Bermudez, Thin Solid Films 343/344 (1999) 476.
[14] B.E. Yodas, J. Mater. Res. 5 (1990) 1157.
[15] J. Lin, Q. Su, J. Mater. Chem. 5 (1995) 1151.
[16] V. Bermudez, L.D. Carlos, M.C. Duarte, M.M. Silva, C.J.R. Silva, M.J. Smith, M. Assuncao, L. Alcacer, J. Alloys Compd. 275–277 (1998) 21.